NeuroImage: Clinical 16 (2017) 205–209

Contents lists available at ScienceDirect

NeuroImage: Clinical

journal homepage: www.elsevier.com/locate/ynicl

A novel method of quantifying brain atrophy associated with age-related hearing loss

Z. Jason Qian[a,1], Peter D. Chang[b,1], Gul Moonis[b], Anil K. Lalwani[a,*]

[a] Columbia University Department of Otolaryngology/Head and Neck Surgery, United States
[b] Columbia University Department of Radiology, United States

ARTICLE INFO

Keywords:
Presbycusis
Age-related hearing loss
Temporal lobe atrophy
Brain atrophy

ABSTRACT

A growing body of evidence has shown that a relationship between age-related hearing loss and structural brain changes exists. However, a method to measure brain atrophy associated with hearing loss from a single MRI study (i.e. without an interval study) that produces an independently interpretable output does not. Such a method would be beneficial for studying patterns of structural brain changes on a large scale. Here, we introduce our method for this.

Audiometric evaluations and mini-mental state exams were obtained in 34 subjects over the age of 80 who have had brain MRIs in the past 6 years. CSF and parenchymal brain volumes (whole brain and by lobe) were obtained through a novel, fully automated algorithm. Atrophy was calculated by taking the ratio of CSF to parenchyma. High frequency hearing loss was associated with disproportional temporal lobe atrophy relative to whole brain atrophy independent of age ($r = 0.471$, $p = 0.005$). Mental state was associated with frontoparietal atrophy but not to temporal lobe atrophy, which is consistent with known results. Our method demonstrates that hearing loss is associated with temporal lobe atrophy and generalized whole brain atrophy. Our algorithm is efficient, fully automated, and able to detect significant associations in a small cohort.

1. Introduction

Presbycusis, or age-related hearing loss (ARHL), is a public health concern of increasing importance with the aging global population. It affects over half of adults over age 75, which is a population expected to double over the next 40 years (Vincent and Velkoff, 2010; Gopinath et al., 2009). ARHL begins with preferential loss of high frequency hearing, with losses progressing into mid and lower frequencies over time. Additionally, the ability to distinguish speech from background noise declines (Gates and Mills, 2005). Hearing loss in the elderly is associated with decreased quality of life through social isolation and dependence on caregivers, increase prevalence of symptoms of depression, and increased overall mortality through falls and accidents (Davis et al., 2016; Arlinger, 2003; Dalton et al., 2003). Furthermore, it is associated with an increased risk of developing dementia (Deal et al., 2017; Lin et al., 2011).

Deficits in the peripheral auditory pathway were initially identified in ARHL; temporal bone histology demonstrated that damage to any of the sensory (outer hair cells), neural (spiral ganglia), or metabolic (stria vascularis) components of the cochlea could contribute to ARHL (Nelson and Hinojosa, 2006; Schuknecht and Gacek, 1993). More recently, attention has been directed towards characterizing structural changes in the central auditory pathway, which lies between the eighth cranial nerve and the cerebral cortex. A growing body of evidence has revealed that hearing loss in the elderly is associated with decreased parenchymal brain volume. For example, one study demonstrated that ARHL is related to smaller total brain volume independent of cognition and cardiovascular risk factors (Rigters et al., 2017), and a longitudinal study showed that elderly subjects with hearing loss have accelerated rates of whole brain and right temporal lobe atrophy (Lin et al., 2014).

Imaging quantification of brain atrophy has already been used extensively to characterize changes in other central pathologies. For example, both visual and quantitative measurements of brain atrophy have diagnostic specificity for detection of Alzheimer's disease (Sullivan et al., 1993; Jobst et al., 1992; de Leon et al., 1989). More recently, brain atrophy has also been used as a biomarker for disease burden in chronic multiple sclerosis (Ge et al., 2000).

Considering the prevalence of ARHL, there exists a high availability of incidentally obtained brain MRIs in affected individuals. The ability to analyze large amounts of this data in an efficient way would improve

* Corresponding author at: Department of Otolaryngology/Head and Neck Surgery, Columbia University College of Physicians and Surgeons, 168 Fort Washington Avenue, Harkness Pavilion 8, New York, NY 10032, United States.
E-mail address: anil.lalwani@columbia.edu (A.K. Lalwani).
[1] Contributed equally to the work.

http://dx.doi.org/10.1016/j.nicl.2017.07.021
Received 26 February 2017; Received in revised form 4 July 2017; Accepted 22 July 2017
Available online 24 July 2017

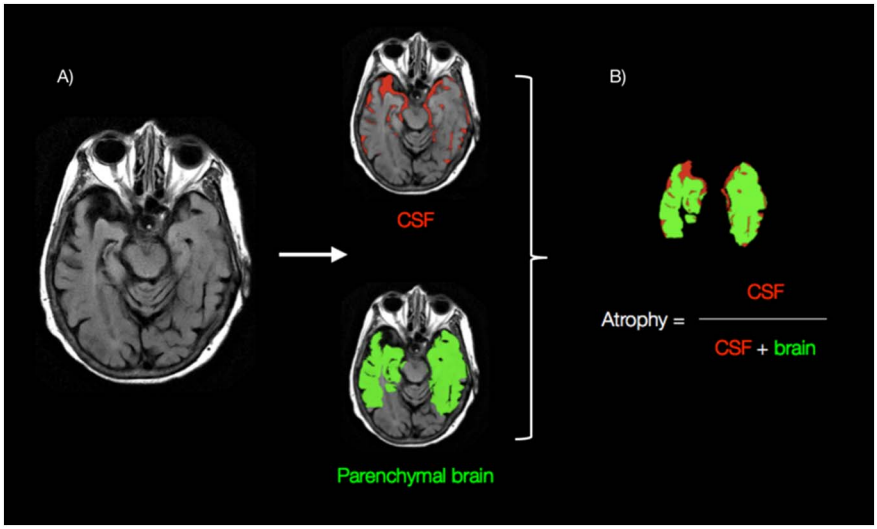

Fig. 1. Quantitative analysis. A) Shown is an axial FLAIR image at the level of the temporal love. A fully automated computer algorithm is used to identify the temporal loves, with further delineation between parenchymal brain volume (green) and the surrounding CSF. B) Quantitative calculation of degree of atrophy is obtained by dividing the volume of CSF by the combined volume of both parenchymal brain volume and CSF. A parallel calculation is also obtained for the whole brain (not just limited to temporal lobes).

understanding of the patterns of structural brain changes related to ARHL. Therefore, we aim to introduce a novel and fully automated software algorithm that measures brain atrophy associated with presbycusis from a single conventional brain MRI without an interval study.

2. Methods

2.1. Subjects

Participants for this cross-sectional study were recruited from the otology clinic at Columbia University Medical Center. The Institutional Review Board of Columbia University approved the protocol and all subjects gave informed consent. Criteria for recruitment included age over 80 years at the time of audiometric evaluation and a brain MRI within 6 years in the medical record. Exclusion criteria included neurodegenerative diseases that may be associated with decreased brain volumes (including Alzheimer's disease, frontotemporal dementia, HIV-related cognitive impairment, Parkinson's disease, and vascular dementia), non-ARHL causes of hearing loss (including retrocochlear pathology, sudden sensorineural hearing loss, and otospongiosis), and history of neurosurgical procedure.

2.2. Audiometry

Measurements were conducted in an audiometric suite using insert earphones and an audiometer calibrated to the standards of the American National Standards Institute (ANSI S3.6-2010). Pure-tone air conduction thresholds were recorded in decibel hearing level (dB HL) units at the following frequencies: 0.25, 0.5, 2, 3, 4, 6, and 8 kHz. The average of all thresholds was taken for each ear on every subject, and the side with the lower average was designated the better hearing ear. High frequency pure-tone averages (HFPTAs) were calculated using thresholds from 3–8 kHz, while low frequency pure-tone averages (LFPTAs) were calculated using thresholds from 0.25–2 kHz.

2.3. Mental status

The mini-mental state exam (MMSE) is a widely-used screen of cognitive ability that incorporates multiple cognitive domains, including orientation, attention, learning, calculation, working memory, and visual construction that is administered through verbal and written commands (Folstein et al., 1975). The test was administered by a research assistant experienced in working with the elderly patients with hearing loss to ensure that all instructions were heard and understood. A score of 30 represents the maximum testable mental status. The reciprocal of the score was used so that better performance (lower reciprocal score) would have a positive correlation coefficient with less brain atrophy.

2.4. Imaging acquisition and analysis

All images were obtained on one of two 3.0 T MRI systems (Signa, GE Healthcare) using an 8-channel head array coil over a 6-year period. As part of standard institutional protocol, an axial fluid-attenuated inversion recovery (FLAIR) acquisition was obtained with the following parameters: TR 9500 ms/TE 127 ms; TI 2250 ms; slice thickness 5 mm with no gap; FOV 225 mm. A histogram normalization algorithm was used to standardize intensity values between patients and to facilitate robust intensity-based tissue classification described below. The method for histogram normalization is based on a technique previously described that maximizes the cross-correlation between cumulative histogram distribution functions of each input volume with a reference standard (Shapira et al., 2013). The reference volume for histogram normalization was a standardized template of 366 normal subjects from the Genetics of Brain Structure and Function Study (Winkler et al., 2012).

A fully automated software algorithm was then used to quantify volumetric parenchymal atrophy within the whole brain and further subdivided into each lobe by hemisphere. The algorithm is implemented sequentially by using a multimodal model for whole brain segmentation followed by intensity-based tissue classification and atrophy calculation (Fig. 1). In brief, whole brain segmentation proceeds by first determining the voxel-wise probability distribution of intracranial boundaries. The T1-weighted, T2-weighted and diffusion-weighted intensity values of each voxel are passed to a single hidden layer neural network trained to differentiate between intra-axial and extra-axial tissues. This initial estimate is then post-processed with a deformable mesh model that finalizes the whole brain mask (Fischl et al., 1999), regularizing the initial estimates to take into account the expected global features and anatomy of the brain.

From the algorithm-generated whole brain mask, a finite mixture model-based method sensitive to intensity scale changes is then used to separate the intracranial contents into two components: brain parenchyma (grey matter, white matter) and CSF (Lundervold and Storvik, 1995). This algorithm classifies brain tissue type by modeling each expected subpopulation (brain parenchyma, CSF) as a Gaussian distribution of intensity values (e.g. Gaussian distribution with low T1/high T2 peak is CSF while the other Gaussian distribution with intermediate T1/T2 peak is brain parenchyma). Subsequently a normalized ratio for brain atrophy to be calculated by dividing volume of CSF by

the combined volume of both parenchymal brain and CSF (Fig. 1B). This normalized metric, which parallels the percentage of intracranial volume composed of CSF, is similar to other validated quantitative measures for volume loss (Ge et al., 2000). From whole brain calculations, lobar specific atrophy estimates for each hemisphere (left and right) are determined using linear co-registration of anatomically labeled MNI152 templates from McConnell Brain Imaging Institute onto each individual patient brain (Collins et al., 1999). Co-registration and downstream calculations were performed automatically as part the image processing pipeline using FMRIB's Linear Image Registration Tool (Jenkinson et al., 2002). The linear affine transformation was implemented using 12 degrees of freedom, trilinear interpolation, and a mutual information cost function.

2.5. Statistical analysis

The statistical software Stata (version 14.1, StataCorp LP, College Station, TX) was used to conduct the analysis. Only the audiometric data of the better hearing ears was analyzed so there would be negligible compensation from the contralateral ears. Statistical dependence between hearing level and brain atrophy was assessed using Pearson correlations (r) due to the normal distributions of hearing thresholds and brain atrophy in the sample. In contrast, statistical dependence between mental status and brain atrophy was assessed with Spearman rank correlations (ρ) due to the scoring ceiling of the MMSE. To investigate the possibility that brain atrophy may independently correlate to hearing level despite both variables being correlated with age, a multiple linear regression analysis with an interaction factor between hearing and brain volume was performed.

3. Results

The mean age of the 34 subjects was 85.5 years (SD = 4.6) at the time of audiometry and 83.2 years (SD = 4.5) at the time of brain MR imaging. The average difference in years between audiometry and brain MR imaging was 2 years (SD = 2.1). The study population was comprised of 23 women (67.6%) and 11 men (32.4%). The entire study population exhibited sensorineural hearing loss (Table 1). In general, advanced age was associated with poorer hearing and greater temporal lobe volume loss, but not with whole brain volume loss or the ratio of temporal lobe to whole brain atrophy.

3.1. Hearing level and brain atrophy

HFPTA was correlated to temporal lobe atrophy ($r = 0.471$, $p = 0.005$, Fig. 2). However, HFPTA was not correlated to whole brain ($r = 0.250$, $p = 0.2$), frontal lobe ($r = -0.024$, $p = 0.9$), parietal lobe ($r = -0.005$, $p = 1.0$), occipital lobe ($r = 0.086$, $p = 0.6$), or cerebellar ($r = 0.116$, $p = 0.5$) atrophy. LFPTA was not correlated to any measures of brain atrophy. Normal probability plots showed that all measures of hearing and brain atrophy in the sample were normally distributed.

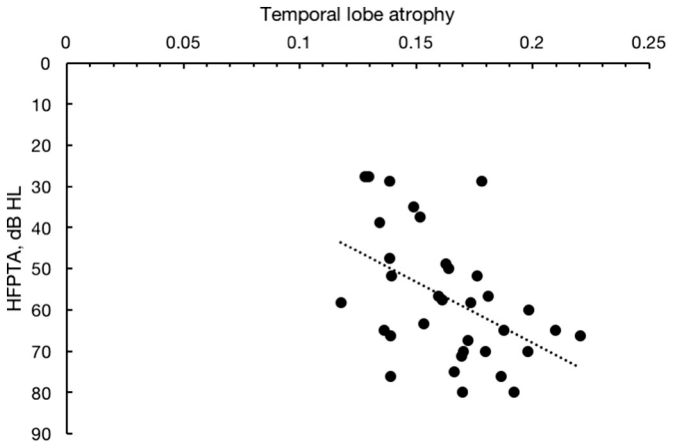

Fig. 2. Correlation between temporal lobe atrophy and high frequency pure tone averages (HFPTA). Higher HFPTAs represent worse hearing ($r = 0.471$, $p = 0.005$).

The ratio of temporal lobe to whole brain atrophy, which represents disproportional temporal lobe volume loss, was correlated to HFPTA ($r = 0.369$, $p = 0.032$, Fig. 3) but not to age ($r = 0.252$, $p = 0.2$).

Temporal lobe atrophy was also correlated with age ($r = 0.358$, $p = 0.038$), however, a multiple linear regression analysis to predict age based on HFPTA and temporal lobe atrophy with a continuous interaction between the latter two variables demonstrated a significant regression equation $F(1, 32) = 14.97$, $p = 0.001$, with an R^2 of 0.32. Therefore, temporal lobe atrophy cannot be directly attributed to age alone.

3.2. Mental status and brain atrophy

MMSE was correlated to whole brain atrophy ($\rho = 0.401$, $p = 0.019$, Fig. 4), frontal lobe atrophy ($\rho = 0.395$, $p = 0.021$), and parietal lobe atrophy ($\rho = 0.393$, $p = 0.021$). However, MMSE was not correlated to temporal lobe atrophy ($\rho = 0.268$, $p = 0.1$), occipital lobe ($\rho = 0.227$, $p = 0.2$), or cerebellar atrophy ($\rho = 0.155$, $p = 0.4$). MMSE score was not correlated to age in this sample ($\rho = 0.301$,

Table 1
Summary of the study population. Of note, ears with mixed hearing loss were included in the study because all had a significant sensorineural component relative to a mild conductive component (< 20 dB HL air-bone gap).

	Total (n = 34)	Age 80–84 (n = 14)	Age 85–89 (n = 15)	Age 90–94 (n = 3)	Age ≥ 95 (n = 2)
Hearing loss, total ears					
Sensorineural	58	22	28	3	3
Conductive	0	0	0	0	0
Mixed	9	3	2	3	1
No hearing loss	0	0	0	0	0
HFPTA, dB HL ± SD					
Better ears	57.3 ± 15.7	48.8 ± 17.3	60.9 ± 11.3	72.1 ± 10.6	67.3 ± 12.7
Worse ears	70.9 ± 32.5	56.5 ± 18.8	81.1 ± 41.1	86.7 ± 24.3	71.5 ± 13.8
LFPTA, dB HL ± SD					
Better ears	38.9 ± 14.8	31.2 ± 15.4	41.7 ± 12.0	48.3 ± 17.6	48.3 ± 14.1
Worse ears	47.9 ± 22.8	37.0 ± 17.2	52.3 ± 20.0	74.4 ± 41.9	50.8 ± 10.6
Brain atrophy ± SD					
Temporal lobe	0.164 ± 0.025	0.195 ± 0.016	0.208 ± 0.020	0.233 ± 0.036	0.197 ± 0.010
Whole brain	0.204 ± 0.022	0.152 ± 0.023	0.170 ± 0.024	0.176 ± 0.032	0.180 ± 0.010
TL/WB ratio	0.803 ± 0.101	0.782 ± 0.109	0.818 ± 0.093	0.757 ± 0.080	0.914 ± 0.001

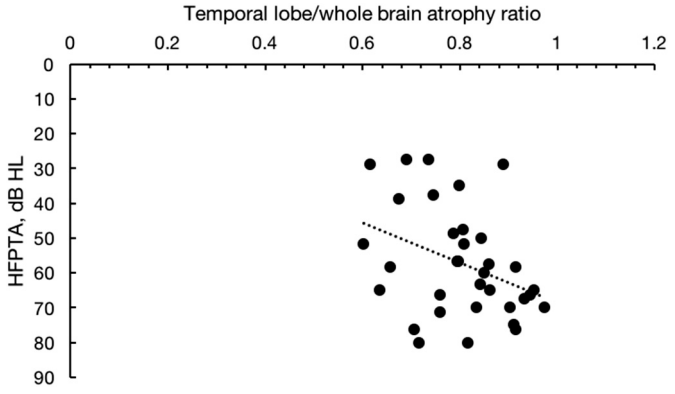

Fig. 3. Correlation between temporal lobe atrophy to whole brain atrophy ratio and high frequency pure tone averages (HFPTA). Higher ratios represent a greater discordance in temporal lobe volume loss relative to whole brain loss. Higher HFPTAs represent worse hearing (r = 0.369, p = 0.032).

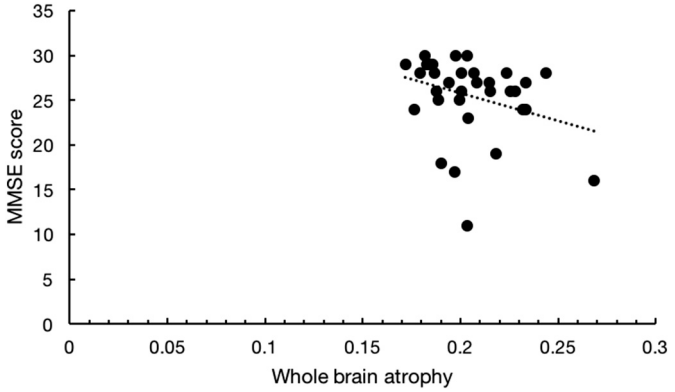

Fig. 4. Correlation between whole brain atrophy and mini-mental state examination (MMSE) score. Higher MMSE scores represent better cognitive function (ρ = 0.401, p = 0.019).

p = 0.08).

4. Discussion

4.1. Hearing and brain atrophy

When considering structural brain changes, it is first important to distinguish normal brain aging from pathologic processes. While recent work has suggested that brain volume loss may be associated with normal aging (Fjell et al., 2013), isolated temporal lobe atrophy is not considered a normal part of aging (Chan et al., 2009; Yankner et al., 2008; Soriani-Lefèvre et al., 2003; Visser et al., 2002).

In the present study, we found that hearing level is correlated with disproportional temporal lobe atrophy relative to whole brain atrophy while age was not. Furthermore, a multiple linear regression analysis of age, HFPTA, and temporal lobe atrophy demonstrated a highly significant interaction between HFPTA and temporal lobe atrophy, indicating that age cannot be attributed to temporal lobe atrophy.

These results support the findings of Lin et al., who found that individuals with peripheral presbycusis experience accelerated rates of atrophy in the auditory cortex (Lin et al., 2014). While a rate was obtained through interval MRI scans, our method can calculate atrophy at single time point using CSF to parenchymal volume ratios based on FLAIR templates and produces complementary results.

Our findings also complement those of Rigters et al., who found that hearing loss is associated with smaller brain volume in a large sample of 2908 participants (Rigters et al., 2017). A cross-sectional comparison of hearing to brain volume obtained through a single MRI is performed in a similar fashion to our study. However, our method calculates brain atrophy, which is an objective value that can be independently interpreted, rather than brain volume alone, which requires relative comparison.

Another key difference is that our method combines grey and white matter for brain parenchymal volume calculations, which reduces the computational time per study. To differentiate grey and white matter, the most robust algorithms consider the respective spatial distributions and require a long processing time. Rigters et al. used a simple K-means algorithm, which shortens computational time but does not consider spatial distribution and sacrifices accuracy, and found no association between grey matter volume and hearing impairment. The limitations of the K-means algorithm should be considered when comparing these results to other studies that found a significant association between grey matter volume and hearing (Eckert et al., 2012; Husain et al., 2011; Peelle et al., 2011). Our method avoids the technical limitations of differentiating grey and white matter volumes in order to detect a significant association between parenchymal brain volume and hearing in a short computational time.

Finally, our results also complement those reported by Fan et al., who detected grey matter auditory cortex volume loss in patients with unilateral sudden hearing loss (Fan et al., 2015). However, there are several key differences in methodology between our algorithm and the SPM software package used in the previous study which primarily relate to approach in normalizing atrophy comparison between patients. Using SPM/DARTEL (Ashburner, 2007), the previous authors could compare GM loss directly by first applying nonlinear co-registration to warp the native brain to match the volume and shape of a default template. However, the process of nonlinear transformation and resulting local distortions in anatomy have the potential to introduce subtle errors in measurement of structural changes, especially given the small but significant 1–2% differences in atrophy between patients demonstrated in this study. By contrast, the methodology of our proposed algorithm calculates atrophy based on brain parenchyma and CSF segmented onto native MRI datasets without warping. In turn comparison of structural changes between patients is accomplished by a relatively novel metric considering the ratio of CSF with relation to entire intracranial contents.

Furthermore, the SPM/DARTEL pipeline involves several steps that require manual user interaction, for example the alignment of anterior/posterior commissures in the process of initial coregistration as well as generation of study-specific patient templates. This is in addition to the downstream high-order nonlinear optimizations that are known to be time and CPU-intensive, usually requiring 1 h or more per single MRI series (Klein et al., 2009). By contrast, our fully automated processing pipeline requires no human interaction and is able generate clinically significant estimates for parenchymal atrophy divided within each lobe of brain in several minutes. The ease and speed of quantitative analysis facilitates the potential widespread adoption of this and other proposed imaging biomarkers in routine practice.

4.2. MMSE score and brain atrophy

The MMSE was included in this study as a method to validate our method of brain atrophy quantification. The rationale is that performance on the MMSE is sensitive to whole brain atrophy and has been mapped to depend on widely distributed cortical areas in bilateral frontal and parietal lobes (Fjell et al., 2009; Apostolova et al., 2006). Therefore, poorer performance on the MMSE should correlate with increased brain atrophy. As expected, our results show that lower MMSE scores were correlated to whole brain, frontal lobe, and parietal lobe atrophy, but not temporal lobe atrophy.

Age is related to MMSE performance; however, these variables were not correlated in the present sample. This is likely due to the relatively homogenous age of our sample. Previous studies that establish norms for MMSE performance categorize subjects by decade of life and show

that the normal range for MMSE scores decreases by decade (Ishizaki et al., 1998; Mungas et al., 1996; Crum et al., 1993). In our sample, the vast majority of subjects are in the ninth decade of life. Therefore, the age range within our sample is likely too narrow to detect a significant correlation with MMSE. It is possible that a correlation could be detected using a larger sample size.

4.3. Weaknesses and limitations

Distinguishing the effects of ARHL on brain atrophy from age alone is difficult. Since both age and hearing loss correlated with brain atrophy, we used a regression analysis to demonstrate that brain atrophy could not be directly attributed to age due to a significant interaction between hearing loss and brain atrophy. In the future, a control group consisting of a younger population with and without hearing loss would be necessary to fully distinguish the effects of age and hearing loss on brain atrophy.

The effects of the temporal relationship between the MRI and audiometry is unclear. Here we demonstrated that significant associations can be made with an average time of 2 years between studies. It is likely that associations would be less significant as the time between MRI and audiometry increases. In the future, a larger cohort should be used to determine the maximum time possible for accurate associations to be made.

4.4. Conclusions

We introduced a new technique to quantify brain atrophy that is highly efficient and robust enough to detect a significant association with hearing in a small cohort. This method revealed that ARHL is associated with temporal lobe atrophy and generalized whole brain atrophy. Our results add to the cumulating evidence that ARHL is associated with structural brain changes. Additional research in this topic is needed to find the mechanistic pathways affected by aging and ultimately identify therapeutic targets.

References

Apostolova, L.G., Lu, P.H., Rogers, S., Dutton, R.A., Hayashi, K.M., Toga, A.W., Cummings, J.L., Thompson, P.M., 2006. 3D mapping of mini-mental state examination performance in clinical and preclinical Alzheimer disease. Alzheimer Dis. Assoc. Disord. 20, 224–231.

Arlinger, S., 2003. Negative consequences of uncorrected hearing loss—a review. Int. J. Audiol. 42 (Suppl. 2) (2S17–20).

Ashburner, J., 2007. A fast diffeomorphic image registration algorithm. NeuroImage 38, 95–113.

Chan, D., Anderson, V., Pijnenburg, Y., Whitwell, J., Barnes, J., Scahill, R., Stevens, J.M., Barkhof, F., Scheltens, P., Rossor, M.N., Fox, N.C., 2009. The clinical profile of right temporal lobe atrophy. Brain 132, 1287–1298.

Collins, L.D., Zijdenbos, A.P., Baaré, W.F.C., Evans, A.C., 1999. ANIMAL + INSECT: improved cortical structure segmentation. In: Information Processing in Medical Imaging. Presented at the Biennial International Conference on Information Processing in Medical Imaging. Springer, Berlin, Heidelberg, pp. 210–223.

Crum, R.M., Anthony, J.C., Bassett, S.S., Folstein, M.F., 1993. Population-based norms for the Mini-Mental State Examination by age and educational level. JAMA 269, 2386–2391.

Dalton, D.S., Cruickshanks, K.J., Klein, B.E.K., Klein, R., Wiley, T.L., Nondahl, D.M., 2003. The impact of hearing loss on quality of life in older adults. Gerontologist 43, 661–668.

Davis, A., McMahon, C.M., Pichora-Fuller, K.M., Russ, S., Lin, F., Olusanya, B.O., Chadha, S., Tremblay, K.L., 2016. Aging and hearing health: the life-course approach. Gerontologist 56 (Suppl. 2), S256–67.

de Leon, M.J., George, A.E., Stylopoulos, L.A., Smith, G., Miller, D.C., 1989. Early marker for Alzheimer's disease: the atrophic hippocampus. Lancet 2, 672–673.

Deal, J.A., Betz, J., Yaffe, K., Harris, T., Purchase-Helzner, E., Satterfield, S., Pratt, S., Govil, N., Simonsick, E.M., Lin, F.R., Health ABC Study Group, 2017. Hearing impairment and incident dementia and cognitive decline in older adults: the health ABC study. J. Gerontol. A Biol. Sci. Med. Sci. 72, 703–709.

Eckert, M.A., Cute, S.L., Vaden Jr., K.I., Kuchinsky, S.E., Dubno, J.R., 2012. Auditory cortex signs of age-related hearing loss. J. Assoc. Res. Otolaryngol. 13, 703–713.

Fan, W., Zhang, W., Li, J., Zhao, X., Mella, G., Lei, P., Liu, Y., Wang, H., Cheng, H., Shi, H., Xu, H., 2015. Altered contralateral auditory cortical morphology in unilateral sudden sensorineural hearing loss. Otol. Neurotol. 36, 1622–1627.

Fischl, B., Sereno, M.I., Dale, A.M., 1999. Cortical surface-based analysis. II: inflation, flattening, and a surface-based coordinate system. NeuroImage 9, 195–207.

Fjell, A.M., Amlien, I.K., Westlye, L.T., Walhovd, K.B., 2009. Mini-mental state examination is sensitive to brain atrophy in Alzheimer's disease. Dement. Geriatr. Cogn. Disord. 28, 252–258.

Fjell, A.M., McEvoy, L., Holland, D., Dale, A.M., Walhovd, K.B., Alzheimer's Disease Neuroimaging Initiative, 2013. Brain changes in older adults at very low risk for Alzheimer's disease. J. Neurosci. 33, 8237–8242.

Folstein, M.F., Folstein, S.E., McHugh, P.R., 1975. “Mini-mental state”. A practical method for grading the cognitive state of patients for the clinician. J. Psychiatr. Res. 12, 189–198.

Gates, G.A., Mills, J.H., 2005. Presbycusis. Lancet 366, 1111–1120.

Ge, Y., Grossman, R.I., Udupa, J.K., Wei, L., Mannon, L.J., Polansky, M., Kolson, D.L., 2000. Brain atrophy in relapsing-remitting multiple sclerosis and secondary progressive multiple sclerosis: longitudinal quantitative analysis. Radiology 214, 665–670.

Gopinath, B., Rochtchina, E., Wang, J.J., Schneider, J., Leeder, S.R., Mitchell, P., 2009. Prevalence of age-related hearing loss in older adults: Blue Mountains Study. Arch. Intern. Med. 169, 415–416.

Husain, F.T., Medina, R.E., Davis, C.W., Szymko-Bennett, Y., Simonyan, K., Pajor, N.M., Horwitz, B., 2011. Neuroanatomical changes due to hearing loss and chronic tinnitus: a combined VBM and DTI study. Brain Res. 1369, 74–88.

Ishizaki, J., Meguro, K., Ambo, H., Shimada, M., Yamaguchi, S., Hayasaka, C., Komatsu, H., Sekita, Y., Yamadori, A., 1998. A normative, community-based study of Mini-Mental State in elderly adults: the effect of age and educational level. J. Gerontol. B Psychol. Sci. Soc. Sci. 53, P359–63.

Jenkinson, M., Bannister, P., Brady, M., Smith, S., 2002. Improved optimization for the robust and accurate linear registration and motion correction of brain images. NeuroImage 17, 825–841.

Jobst, K.A., Smith, A.D., Szatmari, M., Molyneux, A., Esiri, M.E., King, E., Smith, A., Jaskowski, A., McDonald, B., Wald, N., 1992. Detection in life of confirmed Alzheimer's disease using a simple measurement of medial temporal lobe atrophy by computed tomography. Lancet 340, 1179–1183.

Klein, A., Andersson, J., Ardekani, B.A., Ashburner, J., Avants, B., Chiang, M.-C., Christensen, G.E., Collins, D.L., Gee, J., Hellier, P., Song, J.H., Jenkinson, M., Lepage, C., Rueckert, D., Thompson, P., Vercauteren, T., Woods, R.P., Mann, J.J., Parsey, R.V., 2009. Evaluation of 14 nonlinear deformation algorithms applied to human brain MRI registration. NeuroImage 46, 786–802.

Lin, F.R., Metter, E.J., O'Brien, R.J., Resnick, S.M., Zonderman, A.B., Ferrucci, L., 2011. Hearing loss and incident dementia. Arch. Neurol. 68, 214–220.

Lin, F.R., Ferrucci, L., An, Y., Goh, J.O., Doshi, J., Metter, E.J., Davatzikos, C., Kraut, M.A., Resnick, S.M., 2014. Association of hearing impairment with brain volume changes in older adults. NeuroImage 90, 84–92.

Lundervold, A., Storvik, G., 1995. Segmentation of brain parenchyma and cerebrospinal fluid in multispectral magnetic resonance images. IEEE Trans. Med. Imaging 14, 339–349.

Mungas, D., Marshall, S.C., Weldon, M., Haan, M., Reed, B.R., 1996. Age and education correction of Mini-Mental State Examination for English and Spanish-speaking elderly. Neurology 46, 700–706.

Nelson, E.G., Hinojosa, R., 2006. Presbycusis: a human temporal bone study of individuals with downward sloping audiometric patterns of hearing loss and review of the literature. Laryngoscope 116, 1–12.

Peelle, J.E., Troiani, V., Grossman, M., Wingfield, A., 2011. Hearing loss in older adults affects neural systems supporting speech comprehension. J. Neurosci. 31, 12638–12643.

Rigters, S.C., Bos, D., Metselaar, M., Roshchupkin, G.V., Baatenburg de Jong, R.J., Ikram, M.A., Vernooij, M.W., Goedegebure, A., 2017. Hearing impairment is associated with smaller brain volume in aging. Front. Aging Neurosci. 9, 2.

Schuknecht, H.F., Gacek, M.R., 1993. Cochlear pathology in presbycusis. Ann. Otol. Rhinol. Laryngol. 102, 1–16.

Shapira, D., Avidan, S., Hel-Or, Y., 2013. Multiple histogram matching. In: 2013 IEEE International Conference on Image Processing, pp. 2269–2273.

Soriani-Lefèvre, M.-H., Hannequin, D., Bakchine, S., Ménard, J.-F., Manrique, A., Hitzel, A., Kotzki, P.-O., Boudousq, V., Vera, P., 2003. Evidence of bilateral temporal lobe involvement in primary progressive aphasia: a SPECT study. J. Nucl. Med. 44, 1013–1022.

Sullivan, E.V., Shear, P.K., Mathalon, D.H., Lim, K.O., Yesavage, J.A., Tinklenberg, J.R., Pfefferbaum, A., 1993. Greater abnormalities of brain cerebrospinal fluid volumes in younger than in older patients with Alzheimer's disease. Arch. Neurol. 50, 359–373.

Vincent, G.K., Velkoff, V.A., 2010. The Next Four Decades The Older Population in the United States: 2010 to 2050 [WWW Document]. United States Census Bureau. https://www.census.gov/prod/2010pubs/p25-1138.pdf (web archive link, 07 May 2017) (accessed 5.7.17).

Visser, P.J., Verhey, F.R.J., Hofman, P.A.M., Scheltens, P., Jolles, J., 2002. Medial temporal lobe atrophy predicts Alzheimer's disease in patients with minor cognitive impairment. J. Neurol. Neurosurg. Psychiatry 72, 491–497.

Winkler, A.M., Kochunov, P., Glahn, D.C., 2012. FLAIR Templates [WWW Document]. Brainder. https://brainder.org/download/flair/ (web archive link, 07 May 2017) (accessed 5.7.17).

Yankner, B.A., Lu, T., Loerch, P., 2008. The aging brain. Annu. Rev. Pathol. 3, 41–66.